Biosensors and Bioelectronics 46 (2013) 48–52

Contents lists available at SciVerse ScienceDirect

Biosensors and Bioelectronics

journal homepage: www.elsevier.com/locate/bios

Short communication

# High-speed integrated optical logic based on the protein bacteriorhodopsin

Anna Mathesz [a], László Fábián [a], Sándor Valkai [a], Daniel Alexandre [b,c], Paulo V.S. Marques [b,d], Pál Ormos [a], Elmar K. Wolff [e], András Dér [a,*]

[a] Institute of Biophysics, Biological Research Centre of the Hungarian Academy of Sciences, PO Box 521, 6701 Szeged, Hungary
[b] INESC-Porto, Rua do Campo Alegre 687, 4169-007 Porto, Portugal
[c] Universidade de Trás-os-Montes e Alto-Douro, Apartado 1013, 5001-801 Vila Real, Portugal
[d] Departamento de Física e Astronomia, Faculdade de Ciências, Universidade do Porto, Rua do Campo Alegre 687, 4169-007 Porto, Portugal
[e] Institute for Applied Biotechnology and System Analysis at the University of Witten/Herdecke, Herrhausenstrasse 44, 58455 Witten, Germany

A R T I C L E  I N F O

*Article history:*
Received 27 November 2012
Received in revised form
4 February 2013
Accepted 6 February 2013
Available online 24 February 2013

*Keywords:*
Integrated optics
Logic gate
Fast switching
Bacteriorhodopsin

A B S T R A C T

The principle of all-optical logical operations utilizing the unique nonlinear optical properties of a protein was demonstrated by a logic gate constructed from an integrated optical Mach–Zehnder interferometer as a passive structure, covered by a bacteriorhodopsin (bR) adlayer as the active element. Logical operations were based on a reversible change of the refractive index of the bR adlayer over one or both arms of the interferometer. Depending on the operating point of the interferometer, we demonstrated binary and ternary logical modes of operation. Using an ultrafast transition of the bR photocycle (BR-K), we achieved high-speed (nanosecond) logical switching. This is the fastest operation of a protein-based integrated optical logic gate that has been demonstrated so far. The results are expected to have important implications for finding novel, alternative solutions in all-optical data processing research.



## 1. Introduction

Photonics is considered to be a complementary of conventional electronics in future informational technology applications. Instead of electronic conductors and transistors, their optical analogues, miniature light guides and optical switches, respectively, serve as passive and active elements to process (optically coded) information in photonic integrated circuits. One of the biggest challenge is to find proper nonlinear optical (NLO) materials that are able to actively control the flow of information in these optical circuits. Several inorganic and organic materials have been considered for this special application requiring high speed, sensitivity, reliability and log-term stability, however, so far none of them is regarded as the optimal solution. In 2002, we suggested a biomaterial, the protein bacteriorhodopsin (bR), to be used as an NLO material in integrated optical (IO) applications (Ormos et al., 2002), and demonstrated an IO switching and modulation using a bR adlayer on a grating-coupled planar optical waveguide. bR had long been considered as the most promising material in bioelectronics, including, e.g., diverse optical applications (Dér and Keszthelyi, 2001; Oesterhelt et al., 1991; Roy et al., 2004; Stuart et al., 2001; Vsevolodov, 1998). However, Ref. Ormos et al. (2002) was the first demonstration of its use in integrated optics, and inspired a number of upcoming research papers dealing with the application of bR in different optical switch structures, like a fiber-optic ring resonator (Roy et al., 2010; Singh and Roy, 2003; Topolancik and Vollmer, 2006, 2007), an IO Mach–Zehnder (MZ) interferometer (Dér et al., 2007, 2010; Wolff and Dér, 2010; Fábián et al., 2010) or grating coupler (Fábián et al., 2011, 2010). The creation of logical gates and circuits based on microsecond-scale switching with bR combined with a special fiber-optic ring resonator structure has been recently suggested (Roy et al., 2010; Singh and Roy, 2003; Topolancik and Vollmer, 2006, 2007). Despite its theoretical values, the latter realization has to face serious limitations from the practical point of view. It works in watery environment only, the fiber optics are not integrated, and the speed of operation of the logic gate (switching in the 10-microsecond range, using the "BR-M" transition of the bR photoreaction cycle) is far from being competitive with the state-of-the-art integrated optical solutions. In the course of recent developments, however, we have demonstrated several orders of magnitude faster (nano- and subpicosecond) all-optical switching by bR, using real IO structures (MZ interferometer and grating coupler) (Fábián et al., 2010, 2011). In these experiments, the picosecond BR-K and the subpicosecond BR-I transitions of the bR photocycle were utilized. Based on these grounds, here we report on bR-based logic gates

* Corresponding author. Tel.: +36 62 599606; fax: +36 62 433133.
*E-mail address:* derandra@brc.hu (A. Dér).

0956-5663/$ - see front matter 
http://dx.doi.org/10.1016/j.bios.2013.02.022

built around an IO MZ interferometer structure, as suggested in Wolff and Dér (2010). After demonstrating the operation of the gate in different modes (binary and ternary logic) under quasicontinuous illumination conditions, we show how the gate can perform a high-speed logical operation (as a comparator in ternary logic mode, using nanosecond flashes). Possible implications of the results in integrated photonics are discussed.

## 2. Materials and methods

### 2.1. Preparation of the logic device

As a first step, the Mach–Zehnder interferometers (MZI) were prepared by direct laser writing. For the visible light experiments, MZI were drawn by the light of a UV diode laser (405 nm, 120 mW) into a 6–7 μm thick, spincoated photopolymer layer (*NOA81, Norland Optical Adhesives*) on a plasma cleaned coverslide. The nonpolymerized NOA81 was washed away with a 3:1 mixture of acetone and ethanol. The exact procedure of the preparation process was described in Dér et al. (2010). For drawing the MZI for the IR experiments, a frequency-doubled argon laser (244 nm, 20 mW) focussed into a 5–6 μm thick layer of spincoated photopolymerizable hybrid sol–gel deposited on soda-lime glass substrate was used. The non-exposed regions were simply washed away with a solvent (Alexandre et al., 2007). The sol–gel material was methacryloxypropyltrimethoxysilane (MAPTMS) doped with zirconium propoxide (ZPO) in a suitable molar proportion to attain the desired value of refractive index. A cladding layer of the same material but with a different level of zirconium doping was deposited over the device rib structure. The cavity over one arm of the MZI was created by flood exposure through an amplitude mask, by curing the cladding layer except on the cavity region. After dissolution in a solvent, the cavity created exposed the waveguide core on this region over one arm of the interferometer.

A single-mode optical fiber (*Thorlabs 630HP*) was matched to the input and output of the Mach–Zehnder interferometers and fixed to the coverslide. All parts of the structure were fixed to a microscope slide providing the support. A drop of bR suspension (200 μM bR in water) was placed on each arm of the ready-made interferometer and dried for a day at room temperature. As a result, a continuous (30–35 μm thick) layer of bR was formed on the top of the arms of the interferometer.

### 2.2. Experimental setup

The experiments of the all-optical logic device were performed with the setup shown in Fig. 1. The wavelength of the red probe (data) beam laid outside of the absorption band of bR, so as not to excite the sample, while the green pumping (input) beams were able to initiate the bR photocycle. The output fiber was attached to a photomultiplier tube (*Hamamatsu H5784*) and a digital storage oscilloscope (*LeCroy Waverunner 6100A*) was used to record the output signal. The relaxation time of the detecting system was ca. 20 μs. Two types of experiments (quasi-stationary and pump-probe measurements) were performed to demonstrate the versatility of bR-based logical device.

In the quasistationary experiments, the light of a 674 nm continuous wave (CW) diode laser was coupled into the input

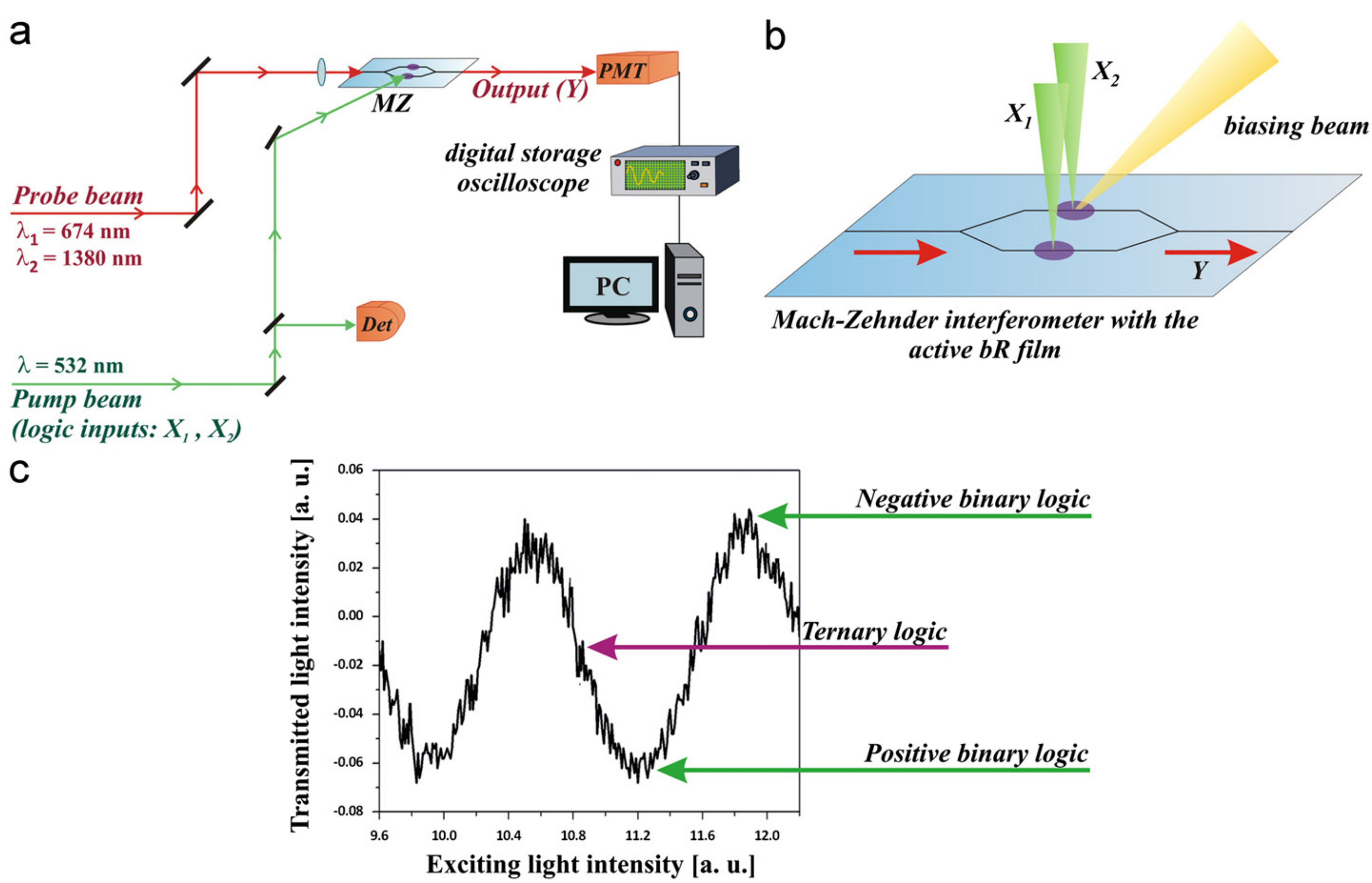


**Fig. 1.** (a) Scheme of the experimental setup used for the quasi-stationary and pump-probe measurements. (b) Schematic representation of the all-optical logic device. (c) Transmission function of the MZ interferometer, and setting of the operating point in the case of binary (two-state) or ternary (tri-state) logic gates.

fiber as a probe beam, while the input values of the logic device were represented by the light of two 532 nm CW diode lasers. Both of the exciting laser beams were split by a glass slide, and the more intense parts of the splitted beams were directed to the bacteriorhodopsin layer, while the other ones were used as reference beams monitored by a photodiode to follow the input characteristics of the logic device.

Pump-probe experiments were also carried out to test our IO switching device, when, instead of quasicontinuous light, short laser pulses representing bits of data were applied. The probe beam in this case was provided by an optical parametric oscillator (OPO) driven by the third harmonic (355 nm) of a *Surelite II-10 Nd:YAG* laser, producing 3.4 ns pulses at 671 nm. Since the incoupling efficiency of the probe strongly depends on the beam quality, the probe beam coming from the OPO was first sent through a beam expander, spatially filtered then directed into the input fiber through a microscope objective. Special care was taken to ensure that the focused intensity remained below the damage threshold of the optical fiber used in the experiments.

The second harmonic beam (532 nm, 5 ns) of the Nd:YAG laser was used to excite the bR sample as a pump beam. In order to avoid damage of the sample, the exciting beam was attenuated by a neutral filter. To be able to excite the two branches of the interferometer independently, small rectangular masks were used. The intensity of probe pulse was measured with and without the exciting light by the photomultiplier.

### 2.3. The operation principle of our device

In our earlier work (Dér et al., 2007), it was shown that a waveguide-based integrated optical Mach–Zehnder interferometer can act as an all-optical light modulator. The active optical component of the device was made of a dried film of bR layered upon the top of the arms of the interferometer. Excitation of the bR film by a continuous laser beam shifts the dynamic equilibrium between the concentrations of the ground state ($BR_{568}$) and the $M_{412}$ intermediate of the bR photocycle, accumulating upon quasi-continuous excitation. (The lower indices refer to the absorption maxima, in nm-s of the corresponding states of the photocycle.) Because of the spectral differences between BR and M, the refractive index of the sample (determined by the ratio of the two states) changes, hence, the effective refractive index of the propagating mode is also altered. When one of the active regions above the interferometer is excited, a phase difference between the two arms develops, consequently, the output intensity changes. Since the ratio of BR and M in the equilibrium mixture depends on the intensity of the continuous-wave excitation, the phase difference between the two arms can be controlled by the exciting light. By a continuous increase of the exciting intensity, a sinusoidal modulation of the output could be observed indicating that, with high enough exciting light, a phase difference higher than $2\pi$ can be achieved (Fig. 1c) (Dér et al., 2010).

#### 2.3.1. Setting the operating point (biasing the interferometer)

Biasing the interferometer, based on the above grounds, was described previously (Dér et al., 2010). The key step is a proper preadjustment of the phase shift of the light propagating in one arm of the MZ interferometer. This can be realized by changing the refractive index of the bR adlayer on one arm via a CW control illumination. Depending on its operating point, the MZ could work as a binary (two-state) or ternary (tri-state) logic gate. If the operating point is set to any of the two extremes of the transmission function, the MZ works as a binary logic gate, while when the operating point is in the middle, the device works as a ternary gate (Fig. 1c). Note that the sensitivity of the interferometer, that is proportional to the first derivative of the transmission function for small signals, is considerably higher in the ternary mode.

## 3. Results and discussion

Since the construction of our logic device allows both binary and ternary modes of operation, first we demonstrated the feasibility of logic gates in these basic modes with experiments using quasi-continuous illumination both for exciting and measuring light beams. Next, we show the results of pump-probe experiments demonstrating how the device can perform a high-speed logical operation as a ternary-logic comparator, using nanosecond laser flashes.

### 3.1. Binary mode

As it was described in the previous section, the input values of our logic device were provided by the quasi-continuous exciting laser beams, while the output was defined by the intensity level of the outcoupled measuring light.

For the input values, the presence of excitation corresponds to logic 1, while the absence of it to logic 0. At the output, logic 1 was represented by high output light intensity of the interferometer, while logic 0 by low one (Fig. 2a).

#### 3.1.1. Inverter

First we tested our device as an inverter (or a NOT gate), the simplest logic gate. We changed an input value ($X_2$) for certain time intervals from 0 to 1, and, as output values, we got 1 and 0, accordingly. Fig. 2b shows the corresponding experimental data.

#### 3.1.2. XOR

As a next step, an XOR gate was realized with our Mach–Zehnder device. First, the operating point of the interferometer was adjusted to a minimum of the transmission function to achieve a binary gate. Afterwards, the branches were excited alternatively or simultaneously. The results and the corresponding truth table of the XOR gate are shown in Fig. 2c and a, respectively.

The above results demonstrate that our bR-based integrated optical device can properly function in the form of various types of logic gates in the binary mode, as was predicted in Wolff and Dér (2010). Since the most widespread applications of photonic switching are related to the telecommunication industry, it was important to demonstrate that the NLO properties of bR allow optical switching also in the telecom wavelength regime (see Fig. S1, Supporting Information).

In the following, we focus on the ternary mode of operation, where the higher sensitivity of the device allows lower input light levels, and faster response times.

### 3.2. Ternary mode

Although, at the dawn of machine computing, ternary logic was considered to be a favourable choice (Glusker et al., 2005), the only modern, electronic ternary computer (Setun) was built in the late 1950, and a newer version in the 1970s (Hunger, 2008). Nowadays, the idea of ternary computing is being revisited, because of its theoretical advantages over binary logic (Connelly, 2008). Given a set of assumptions outlined in Hayes (2001), base *e* is the most efficient base for representing arbitrary numbers. Since in practice the base must be an integer, ternary logic would be more efficient than binary (Dhande and Ingole, 2005; Hurst, 1984). In fact, its advantages have been confirmed in

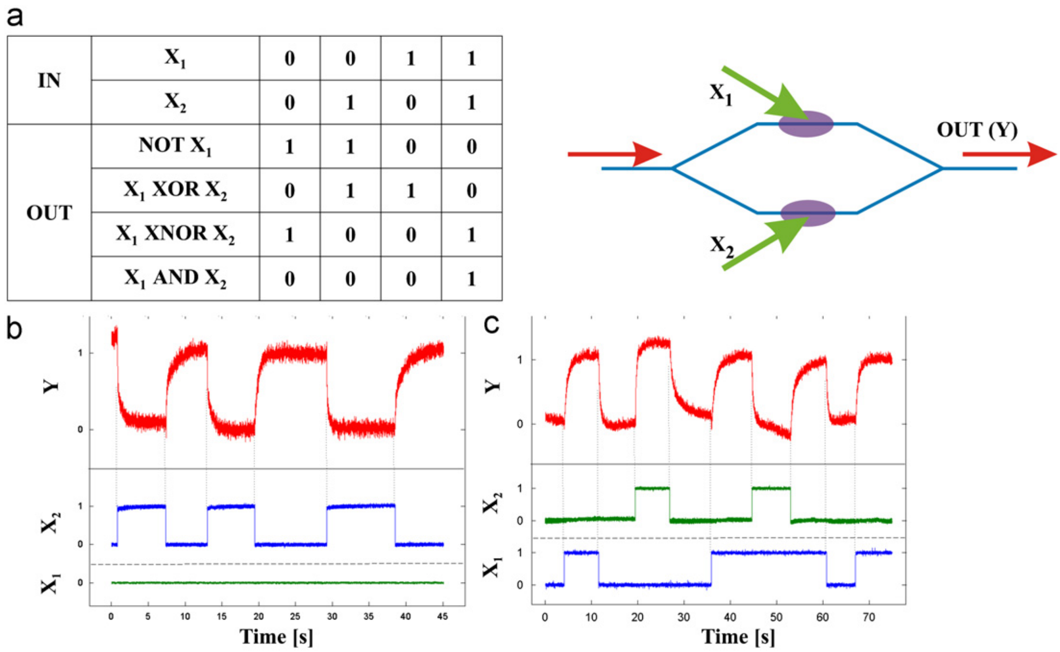


| | | | | | |
|---|---|---|---|---|---|
| IN | $X_1$ | 0 | 0 | 1 | 1 |
| | $X_2$ | 0 | 1 | 0 | 1 |
| OUT | NOT $X_1$ | 1 | 1 | 0 | 0 |
| | $X_1$ XOR $X_2$ | 0 | 1 | 1 | 0 |
| | $X_1$ XNOR $X_2$ | 1 | 0 | 0 | 1 |
| | $X_1$ AND $X_2$ | 0 | 0 | 0 | 1 |

**Fig. 2.** (a) left: Truth table of the basic logical operations in binary mode. right: The logic inputs ($X_1$, $X_2$) and the output of the interferometer (Y). (b) Demonstration of our all-optical logic device working as an inverter. (c) Experimental data of the XOR gate.

digital memories, communications components, and the field of digital signal processing (Wu and Huang, 1993). Despite, the practical realization of ternary computing has still been considered to be a matter of debate (Connelly, 2008).

As a simple but important device working in the ternary logic mode, we realized an integrated optical comparator. In electronics, a comparator is a device that compares two input signals, and indicates at the output, which one is larger. It is easy to see that if the operating point is set to the middle of the sinusoidial transmission function curve (Fig. 1c), our IO device can perform the function of an all-optical comparator. Excitation of each arm leads to phase difference changes with opposite signs, therefore the output intensity changes oppositely in the two cases. Moreover, collective excitation of the arms leads to zero phase change when the output remains unchanged.

In one series of experiments, quasi-continuous illumination was used for the input signals. In Fig. 3a it is shown, that the output light intensity level changes in the opposite direction when alternatively exciting the bR films above the two arms of the interferometer. If, namely, $X_1 > X_2$, the output signal is positive, while if $X_1 < X_2$, it is negative. If the input values are equal ($X_1 = X_2$), the output intensity does not change. Note that the input intensities applied in this case were ca. 3 times smaller than those used during the experiments in the binary mode.

In the next set of experiments, we were utilizing another advantage of using our device in the ternary mode, namely that high sensitivity of our MZ device at the ternary working point (see the discussion under Fig. 1c, Material and Methods) allows to demonstrate a high speed of operation. The optical path difference between the pump and probe beams was carefully adjusted so that they hit the sample at the same time. Taking into account the linear response of the interferometer and the picosecond rise time of the K intermediate, in this case, the speed of the switch is limited by the pulse length of the pump and probe beams. According to our simulations, under the experimental conditions, the 10–90% rise time of the output signal is ca. 8 ns. Strictly speaking, this is the switching speed of the gate, but, in concert with the experimental results, a probe pulse arriving with zero delay at the sample (centered to the midpoint of this rise) already observes a refractive index change that is high enough to allow IO switching (for a detailed description, see Supporting Information). Note that by shortening the pump and probe pulses, one could approach picosecond switching speeds, limited only by the BR-K transition time.

Fig. 3b demonstrates the electric response of the measuring system on intensity changes (Y) of the probe pulse, with the pump pulse exciting the bR film above either or both arms of the interferometer (corresponding to distinct, nonzero $X_1$ and $X_2$, or collective $X_1 + X_2$ inputs). For the sake of better visibility, the probe beam without excitation was subtracted from the signals, so Fig. 3b shows the resulting differential responses. The results clearly demonstrate the operation of the bR-based, fast integrated optical comparator.

## 4. Conclusions and outlook

Using an ultrafast transition of the bR photocycle (BR-K), we realized a high-speed (nanosecond) all-optical logic gate operating in the ternary logic mode. This is the fastest real logical operation of an integrated biophotonic device that has been demonstrated so far. As it has been underpinned by our recent optical switching experiments (Fábián et al., 2011), the ultrafast reaction times of the early intermediates of the bR photocycle (picosecond for K and subpicosecond for I), in principle, allow several orders of magnitude faster logical operations, too. Taking into account the extreme robustness of bR films (cyclicity: $> 10^6$, heat stability until ca. 100 °C, durability: longer than 10 years) (as reviews, see Dér and Keszthelyi, 2001; Vsevolodov, 1998, and references therein), the realization of such ultrafast logic devices may eventually revolutionize all-optical data communication. In addition, our results are expected to contribute to the revival of ternary logic devices, as well, since the implementation of our fast comparator represents a working prototype of an all-optical logic gate operating in ternary mode.

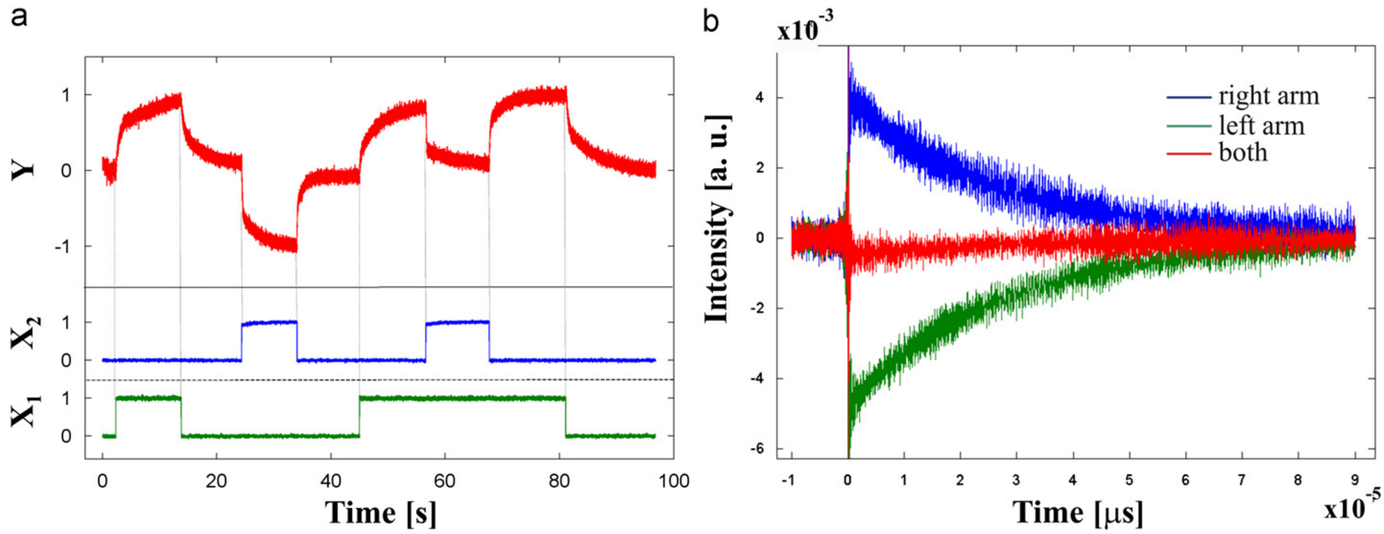


c

| | | | | | |
|---|---|---|---|---|---|
| IN | $X_1$ | 0 | 1 | 0 | 1 |
| | $X_2$ | 0 | 0 | 1 | 1 |
| OUT | Y | 0 | 1 | -1 | 0 |

**Fig. 3.** (a) Experimental data of the all-optical comparator realized as a ternary logic gate. (b) Demonstration of the fast operation mode of the comparator. Intensity change traces measured at the output (Y) of the MZI in the case of distinct ($X_1$ or $X_2$, blue or green, respectively) and collective ($X_1+X_2$, red curve) excitation of the arms of the MZI. Note that, though, the kinetics of the recorded traces were limited by the relaxation time of the electronic detection system (ca. 20 μs), the time resolution of the optical logical device is determined by the ns time course of the pump and probe pulses, as usual in pump-probe experiments (see also in Supporting Information). (c) Truth table of the ternary mode comparator. (For interpretation of the references to color in this figure legend, the reader is referred to the web version of this article.)

## Acknowledgements

This work was supported by Hungarian research grants KTIA-OTKA CK-78367 and TÁMOP-4.2.2.A-11/1/KONV-2012-0060, by an EU networking program COST MP1205, and a Travel grant, DFG WO1713/2-1.

## Appendix A. Supporting information

Supplementary data associated with this article can be found in the online version at http://dx.doi.org/10.1016/j.bios.2013.02.022.

## References

Alexandre, D., Viegas, J., Fernandes, L., Moreira, P.J., Leite, A.M.P., Santos, J.L., Marques, P.V.S., 2007. In: Baldini, F., Homola, J., Lieberman, R.A., Miler, M. (Eds.), Optical Sensing Technology and Applications. Prague, Czech Republic, pp. U168–U179 Spie-Int. Soc. Optical Engineering.
Connelly, J., 2008. Ternary Computing Testbed, 3-Trit Computer Architecture., Computer Engineering Department. California Polytechnic State University of San Luis Obispo.
Dér, A., Keszthelyi, L., 2001. Bioelectronic Applications of Photochromic Pigments. IOS Press, Amsterdam, The Netherlands.
Dér, A., Valkai, S., Fábián, L., Ormos, P., Ramsden, J.J., Wolff, E.K., 2007. Photochemistry and Photobiology 83 (2), 393–396.
Dér, A., Valkai, S., Mathesz, A., Andó, I., Wolff, E.K., Ormos, P., 2010. Sensors and Actuators B: Chemical 151, 26–29.
Dhande, A.P., Ingole, V.T., 2005. Design and implementation of 2 Bit ternary ALU slice, in: SETIT 2005, Third International Conference: Science of Electronic, Technologies of Information and Telecommunications, Tunisia.
Fábián, L., Heiner, Z., Mero, M., Kiss, M., Wolff, E.K., Ormos, P., Osvay, K., Dér, A., 2011. Optics Express 19 (20), 18861–18870.
Fábián, L., Wolff, E.K., Oroszi, L., Ormos, P., Dér, A., 2010. Applied Physics Letters 97, 023305.
Glusker, M., Hogan, D.M., Vass, P., 2005. IEEE Annals of the History of Computing 27 (3), 4–22.
Hayes, B., 2001. American Science 49 (6), 490.
Hunger, F., 2008. SETUN. An Inquiry into the Soviet Ternary Computer. Institut für Buchkunst, Leipzig, Germany.
Hurst, S.L., 1984. IEEE Transactions on Computers 33 (12), 1160–1179.
Oesterhelt, D., Brauchle, C., Hampp, N., 1991. Quarterly Reviews of Biophysics 24, 425–478.
Ormos, P., Fábián, L., Oroszi, L., Ramsden, J.J., Wolff, E.K., Dér, A., 2002. Applied Physics Letters 80, 4060–4062.
Roy, S., Prasad, M., Topolancik, J., Vollmer, F., 2010. Journal of Applied Physics 107, 053115.
Roy, S., Sharma, P., Dharmadhikari, A.K., Mathur, D., 2004. Optics Communication 237, 251–256.
Singh, C.P., Roy, S., 2003. Optics Communication 218, 55–66.
Stuart, J.A., Marcy, D.L., Birge, R.R., 2001. In: Dér, A., Keszthelyi, L. (Eds.), Bioelectronic Applications of Photochromic Pigments. IOS Press, Amsterdam, The Netherlands, pp. 15–29.
Topolancik, J., Vollmer, F., 2006. Applied Physics Letters 89, 184103.
Topolancik, J., Vollmer, F., 2007. Biophysical Journal 92, 2223–2229.
Vsevolodov, N.N., 1998. Biomolecular Electronics. Birkhauser, Boston.
Wolff, E.K., Dér, A., 2010. Nanotechnology Perceptions 6, 1–6.
Wu, C.Y., Huang, H.-Y., 1993. IEEE Journal of Solid-State Circuits 28, 8.